

# Multi-Objective Genetic Algorithm for Civil UAV Path Planning Using 3G Communication Networks



Fan-Hsun Tseng<sup>1</sup>, Cho-Hsuan Lee<sup>2</sup>, Li-Der Chou<sup>1</sup> and Han-Chieh Chao<sup>2,3,4,5</sup>

<sup>1</sup> Department of Computer Science and Information Engineering, National Central University  
Taoyuan 32001, Taiwan, ROC  
fanhsuntseng@ieee.org; cld@csie.ncu.edu.tw

<sup>2</sup> Department of Electronic Engineering, National Ilan University  
I-Lan 26047, Taiwan, ROC  
bruce751227@gmail.com

<sup>3</sup> Department of Computer Science and Information Engineering, National Ilan University  
I-Lan 26047, Taiwan, ROC

<sup>4</sup> Department of Electrical Engineering, National Dong Hwa University  
Hualien 97401, Taiwan, ROC

<sup>5</sup> School of Information Science and Engineering, Fujian University of Technology  
Fuzhou 350118, China  
hcc@niu.edu.tw

Received 7 June 2015; Revised 11 July 2015; Accepted 8 December 2016

**Abstract.** Unmanned Aerial Vehicles (UAVs) have been extensively applied to various applications, such as military aircraft exploration, image transmission for dangerous terrain, relief of disaster. In general, civil UAVs utilize satellite, Global Positioning System, Wi-Fi or the third generation of mobile telecommunications (3G) for data transmission. However, the transmission range of above-mentioned communication technologies limits the flight route of civil UAVs. In this paper, we utilize 3G communication networks for data transmission of civil UAVs. We proposed the multi-objective Genetic algorithm (MOGA) to maximize received signal strength and minimize the path length of flight route. In our simulation-based analysis, the proposed MOGA is superior to the previous proposed signal-greedy and path-greedy algorithms. The simulation results show that the proposed MOGA yields the 1.32 and 3.22 times better signal quality compared to signal-greedy and path-greedy algorithms.

**Keywords:** 3G, civil unmanned aerial vehicle, genetic algorithm, multi-objective optimization, path planning

## 1 Introduction

An Unmanned Aerial Vehicle (UAV) [1] is an aircraft without any pilot in the vehicle. It is simply controlled by ground crew, control tower and navigation system [2] to pilot vehicle automatically. According to functionalities and features, the taxonomy of UAV can be roughly classified into 6 categories, which are attacking on target, terrain exploration [3], air battle and combat, logistics, research and development for civil [4] and commercial purposes. UAV has been widely applied to a great quantity of applications, such as battlefield, disaster field, and civil usage. In the U.S., the well-developed global satellites and ground stations benefit the communication capability for civil UAVs. UAVs not only go on flight missions but also transmit real-time image and data to ground stations. Unlike using the satellite communication in the U.S., UAV transmits its exploration data based on fixed ground wireless

transceiver in Taiwan. Therefore, telemetry and exploration are restricted to the communication coverage of transceiver.

In order to solve the expensive satellite transmission and unsatisfied communication coverage, we investigate the path planning problem of civil UAV by using the third generation of mobile communication (3G) networks in this paper. The base stations (BSs) of 3G networks are well constructed and deployed. Once the flight route is covered by the signal coverage of BS, remote controllers are able to receive information from UAV. Civil UAVs using 3G networks not only extends flight range but also economize construction cost without deploying new infrastructures. However, the inherent coverage hole problem [5] exists in mobile communications. Therefore, we proposed a multi-objective Genetic algorithm (MOGA) for civil UAV path planning using 3G networks.

The remainder of the paper is organized as follows. In section II, background and related technologies are introduced, such as UAVs, civil UAVs, 3G communications, and path planning algorithms. Moreover, the relevant works of civil UAV path planning are also discussed. Section III presents the proposed mechanism, which includes system architecture, flight scenario, path planning with 3G networks, and the proposed MOGA. A path planning case and simulation results are illustrated and analyzed in section IV. Conclusion and future work are given in section V.

## 2 Background and Related Works

### 2.1 UAV and Civil UAV

A UAV as well as a drone stands for a craft or vehicle without any human pilot. It utilizes ground crew and station control or navigation system to simply locate and conduct self-flying. Civil UAVs are different to military UAVs, which are widely applied to some risk and dangerous missions, such as exploration of volcano mountain, avalanche, mudflow and landslide, observation of meteorology and monitoring of gas pipelines [6]. Military UAVs are financed by the military and national defense expenditure. Military UAVs transmit collected information and data by utilizing satellite communication. Civil UAVs are supported by some companies, enterprises and forums. Civil UAVs usually use radio frequency transceivers to replace expensive satellite communication. Nevertheless, civil UAVs are suffered from the communication range of wireless transceivers.

### 2.2 Third Generation of Mobile Telecommunications

The 3G standard is defined by International Telecommunication Union (ITU) and complied with International Mobile Telecommunications-2000 (IMT-2000) specifications. The high data rate mobile communication technologies are provided with voice call, packet data, multimedia applications and instant messaging services. Several well-known technologies are included in 3G standard, such as CDMA2000 (C2K), Wideband Code Division Multiple Access (W-CDMA), Time Division Synchronous Code Division Multiple Access (TD-SCDMA) and Worldwide Interoperability for Microwave Access (WiMAX). IMT-2000 defines that the specification of 3G satisfies 144 and 384 kbps data rate for high and low speed vehicular environment, and 2Mbps for fixed environment. Soft handover technique achieves continuous signal when user leaves its serving BS and approaches target BS. The most valuable improvement is the high-speed data rate in terms of downlink capability.

### 2.3 Path Planning Algorithms

There are various existing algorithms for path planning, such as Dijkstra's algorithm [7], geographical routing algorithm [8], clustering approach [9], particle swarm optimization [10], and A Star search algorithm [11]. A greedy algorithm always selects the best choice in terms of its object at each step and leads to its optimal results, but it may fall into local optimum solution which is shown as Fig. 1 (a). In the example, the value of node represents its payoff. A greedy algorithm chooses the right child in first step because of the bigger payoff. Then, it will choose the right child at second step. As a result, it does not acquire the optimal payoff. The correct solution of this example should be operated as Fig. 1 (b). The global optimum payoff is 100 rather than 24. The node should choose the left child in first step. Then it

selects the left child whose payoff is 100 at second step. It can be observed that a greedy algorithm may fall into a local optimum solution.

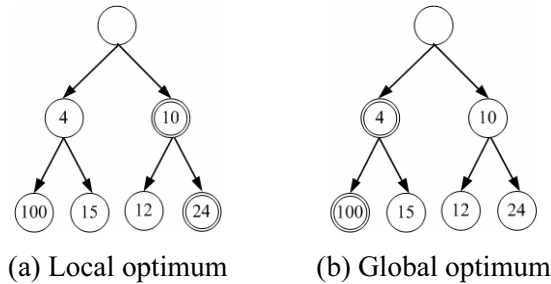


**Fig. 1.** Local optimum and global optimum solutions

The A Star (or simply A\* throughout this paper) search algorithm improves the Dijkstra's algorithm on computation complexity. It adopts the principle of searching optimal solution to form a search tree diagram. A\* algorithm uses heuristic evaluation function to calculate the costs of each neighboring node, which is evaluated as

$$F(n)=G(n)+H(n), \quad (1)$$

where  $G(n)$  is the minimum cost from source node  $S$  to current node  $N$ . The function  $H(n)$  is the minimum cost from current node  $N$  to destination node  $D$ . It maintains an open list array and a close list array. The possible intermediate nodes of current node  $N$  are recorded in the open list array, and traveled nodes are recorded in the close list array. It does not check traveled nodes herein. The operation concept of an A\* algorithm is described as follows. Firstly, the positions of source node  $S$  and destination node  $D$  are known. Then, the neighbor nodes of source node  $S$  are recorded in the open list array. According to the equation (1), it calculates the heuristic evaluation function  $F(n)$  of its neighbor nodes. Lastly, A\* algorithm selects the minimum  $F(n)$  as next current node  $N'$  from the open list array, until it reaches the destination node  $D$ .

#### 2.4 Related Works of Path Planning for UAV

In order to complete missions faultlessly, UAV needs a well-designed flight route. Path planning is vital to both of military UAVs and civil UAVs. The existing and relevant works to UAV path planning are discussed and compared. In [12], UAVs are teamed up to transmit data information with 3G networks. Authors in [13] utilized the BSs of 3G to communicate with ground crew. Authors in [14] designed an enhanced A\* algorithm to plan the flight route of UAV and to avoid the military equipment of the air force. Since UAVs are unable to change flight direction sharply under high mobility, the authors shrink solution space by deleting the impossible flight directions. In addition, the authors consider the fuel of UAV for path planning. The real flight environment of UAV is a three-dimensional (3D) space. Therefore, authors in [15] proposed a 3D path planning approach based on A\* algorithm. Authors in [16] proposed a mechanism named Virtual Force (VF) to dynamically avoid obstacles and overcome the static defect of A\* algorithm. Authors in [17] proposed a 3D offline path planning for UAVs based on multi-objective evolutionary algorithm (MOEA), which is different to the dynamic environment in this work. Authors in [18] investigated the path planning problem of UAV and proposed the immune GA. The proposed immune GA integrates immune algorithm and GA. However, we consider multiple objects and use 3G communication networks for civil UAV in this work. In [19] and [20], the static path planning is different to the dynamic path planning in this work. Moreover, an additional mobile robot is needed in their framework. In [21], the path-greedy and signal-greedy algorithms have been proposed to plan the flight route of civil UAVs. Both of them are able to plan a flight route with 3G communication for civil UAVs instantly. However, the greedy approaches may result in the longer flight path or the worse signal strength. In this paper, we proposed MOGA to optimize both of signal strength and path length for civil UAVs using 3G communication networks. The comparison of existing literatures on UAV path planning is shown in Table 1.

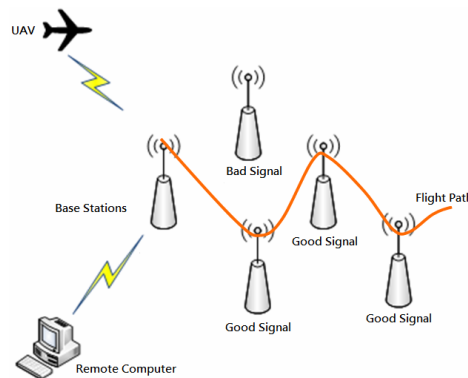
**Table 1.** Comparison of existing literatures.

Papers	Communication	Path Planning	Environment	Number of UAVs
[12]	3G	None	Only 3G BS	More than one
[13]	3G	None	Only 3G BS	One
[14]	Satellite	Enhanced A* algorithm	Static 3D	One
[15]	Satellite	A* algorithm	Static 3D	One
[16]	Satellite	A* algorithm with VF	Dynamic 3D	One
[17]	Satellite	MOEA	Dynamic 3D	One
[18]	Satellite	Immune GA	Static 3D	One
[19][20]	None	MOGA	Static 3D	One Robot
[21]	3G	A* with greedy approach	Dynamic 3D	One
Proposed method	3G	MOGA	Dynamic 3D	One

### 3 Proposed Mechanism

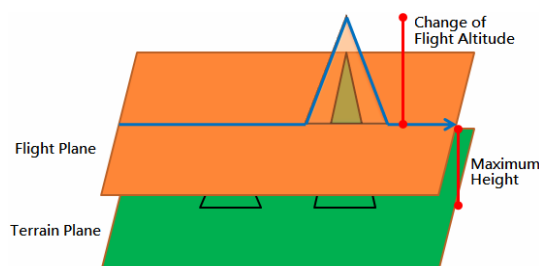
#### 3.1 System Architecture

In this paper, we propose the MOGA for civil UAV path planning using 3G communication networks. The received signal strength of BS is considered as the planning metric of flight route. The continuous signal provides uninterrupted data communication for UAVs. The designed system architecture is shown as Fig. 2. A UAV seeks to find out good signal along its flight path, so that it is able to transmit the collected data to ground crew. The planned flight path is distant from the BS with bad signal.

**Fig. 2.** The designed system architecture of civil UAVs

#### 3.2 Flight Scenario

In order to strengthen and stabilize signal quality, the distance between unmanned aircraft with BSs must be as close as possible. However, the excessively close distance may cause air crash. Therefore, we define a safe flight altitude to prevent collisions. The designed flight scenario is capture in Fig. 3. If an obstacle is higher than the flight plane which means that it exceeds safe flight altitude, UAV must climb up or bypass the obstacle for preventing collisions. After that, it descends and approaches the safe flight altitude.

**Fig. 3.** The designed flight scenario of civil UAVs

### 3.3 Path Planning with 3G Communication Networks

We expect to find out the optimal flight route with the best signal strength and shorter path length. Without loss generality, the shorter distance between UAV and BS leads to stronger signal strength. We refer to the link budget definition from the Telecom Technology Center in Taiwan [22][23], and formulate it to evaluate the link budget of UAV. The free space path loss (FSPL) in dB is shown as equation (2). The detailed variables are given as follows. The variable  $\lambda$  represents wavelength in meter and the variable  $f$  is frequency in hertz. The variable  $d$  represents the distance between UAV and BS, and the unit is meter herein. The variable  $c$  is the velocity of light, and the unit is meters per second.

$$\begin{aligned}
 FSPL &= 10 \log \left( \left( \frac{4\pi d}{\lambda} \right)^2 \right) \\
 &= 20 \log \left( \frac{4\pi d f}{c} \right) \\
 &= \sum_{i=1}^n 20 \log(d(i)) + \sum_{i=1}^n 20 \log(f) + \sum_{i=1}^n 20 \log \left( \frac{4\pi}{c} \right) \\
 &= \sum_{i=1}^n 20 \log \left( \sqrt{(X_{UAV} - X_{BS_i})^2 + (Y_{UAV} - Y_{BS_i})^2 + (Z_{UAV} - Z_{BS_i})^2} \right) + \sum_{i=1}^n 20 \log(f) + \sum_{i=1}^n 20 \log \left( \frac{4\pi}{c} \right)
 \end{aligned} \tag{2}$$

The distance of flight path is calculated by equation (3).

$$Path = \sum_{i=0}^{n-1} \sqrt{(x_i - x_{i-1})^2 + (y_i - y_{i-1})^2 + (z_i - z_{i-1})^2} \tag{3}$$

### 3.4 Multi-Objective Genetic Algorithm

In this paper, the MOGA for civil UAV path planning using 3G communication networks is proposed. The designed operations of proposed GA include encoding, crossover, and mutation operations. Besides, the fitness function of GA is also defined and formulated. In order to apply the evolutionary process of GA to path planning for civil UAV, we formulate a possible flight route as a chromosome. An example of path planning for civil UAV is captured in Fig. 4. An example of planned network topology is transformed as Fig. 4 (a). Each point is regarded as a substring of chromosome. A potential flight path of the example is captured in Fig. 4 (b), where red points present unavailable terrains and dark grey points stand for flight route. Note that red points are unable to be a substring of chromosome during encoding operation, because they are unavailable terrains. We formulate dark grey points as a chromosome as well as a flight route, which is illustrated with Fig. 5.

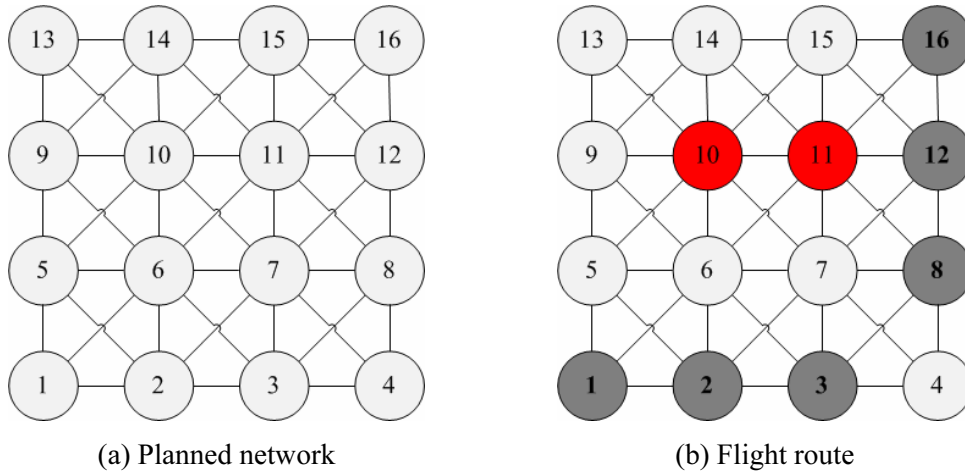


**Fig. 4.** An example of flight path planning

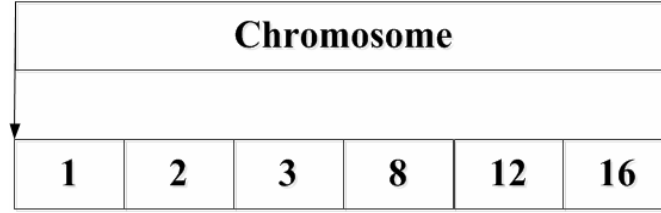


Fig. 5. Illustration of the designed chromosome

Each chromosome has its fitness value for deciding the superiority of an offspring in evolution process. Herein, the fitness value of chromosome is formulated and explained. In the proposed MOGA, both of path cost and signal strength of a flight route are considered. The fitness value of a chromosome is calculated as

$$\text{Fitness value} = \alpha * (\text{Path Cost}) + \beta * (\text{Signal Strength}). \quad (4)$$

$$\alpha + \beta = 1. \quad (5)$$

However, the weight of path cost and signal strength is different. In order to keep the fairness of these two objects, we formalize the equation of fitness value as

$$\text{Fitness value} = \alpha * \left( \frac{\sum_{i=1}^n \text{Path}_{UAV}(i) - \text{Path}_{\min}}{\text{Path}_{\max} - \text{Path}_{\min}} \right) + \beta * \left( \frac{W_{\max} - \frac{\sum_{i=1}^n W_{UAV}(i)}{i}}{W_{\max} - W_{\min}} \right). \quad (6)$$

The function  $\text{Path}_{UAV}(i)$  represents the flight distance from point  $i-1$  to point  $i$ . The variable  $\text{Path}_{\max}$  is the maximum distance of flight path, and the variable  $\text{Path}_{\min}$  is the minimum distance of flight path. The function  $W_{UAV}(i)$  represents the received signal power at point  $i$ . The variables  $W_{\max}$  and  $W_{\min}$  are the maximum and minimum signal power, which are located in the center and at the edge of a BS. Note that the communication radius of BS is 3km.

In initial stage, some available flight paths are encoded as chromosomes and put into mating pool. Then, two chromosomes are selected to crossover for better offspring. In the selection mechanism of proposed GA, we utilize the tournament selection approach to choose two best chromosomes from mating pool according to their fitness values. After that, one point crossover operation is executed. Because each chromosome implies an available flight path, an offspring may be unavailable if there is no limitation in crossover operation. Therefore, the one point crossover must be executed on the same substring of two chromosomes. The designed crossover operation is illustrated with Fig. 6. For instance, chromosomes A and B have the same substring 2, which means that both of these two flight paths pass through the point 2. Then chromosome A and chromosome B exchange their substrings in front of and in back of substring 2. The designed crossover operation guarantees that the offspring 1 and offspring 2 are two available flight routes. After crossover operation, the offspring with better fitness value should be selected and put into group pool for improving the performance of flight path.

The mutation operation is designed for preventing local optimum solutions and also for increasing the diversity of offspring. The designed mutation operation is illustrated with Fig. 7. The one point mutation approach is applied to the designed mutation operation. To avoid acquiring an unavailable flight route, the mutation operation is restricted to an available path between the previous point and next point. For example, mutation point is executed at the substring 2 of chromosome A. The mutation result of offspring is limited to a potential flight route between point 1 and point 3. In this case, the substring 2 of chromosome A is mutated to point 6 and point 7, which is an available flight route between point 1 and point 3. After mutation operation, the fitness value of offspring should be examined whether its fitness value is better than the parent chromosomes or not. If the fitness value is better, it will be put into group pool as a candidate flight route.

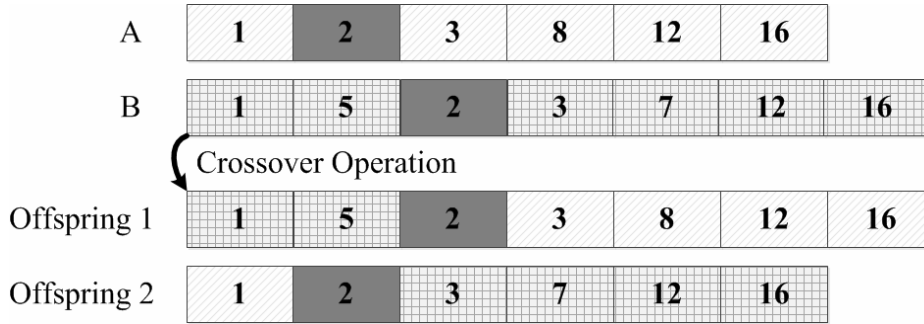


Fig. 6. Illustration of the designed crossover operation

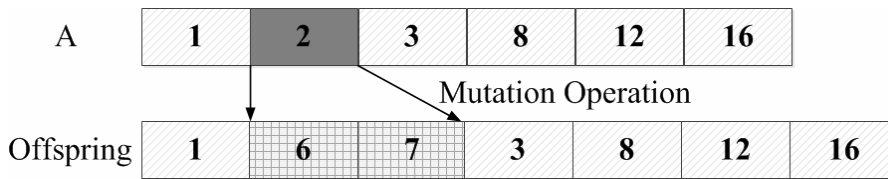


Fig. 7. Illustration of the designed mutation operation.

After encoding, selection, crossover and mutation operations, the designed GA is terminated when it reaches the pre-defined generation number or the fitness value of offspring is unchanged after several generations. Then, the offspring with the best fitness value is regarded as the optimal result of path planning. Therefore, the civil UAV is able to obtain the optimal flight route regarding to the path cost and signal strength.

## 4 Simulation and Analysis

### 4.1 Path Planning Case

Simulation result is performed with MATLAB [24]. The planned map size is the square of 25 kilometers. The coordinate axis of source point  $S$  is (1,1), and the destination point  $D$  is in the coordinate position (20,20). There are 13 BSs and their center coordinate position are (4,4), (5,11), (5,16), (6,6), (10,4), (13,2), (14,16), (15,6), (16,2), (18,11), (18,16), (19,2) and (19,6) respectively. The planned network topology is captured in Fig. 8. The communication radius of each BS is 3 km. There are two mountains where are located at (6,6) and (15,5), and their vertical height are 1.8 and 2.2 km respectively. In the equation of link budget, the wavelength is 1821.5 (MHz) and the speed of light is  $2.99792458 \times 10^8$  (m/s).

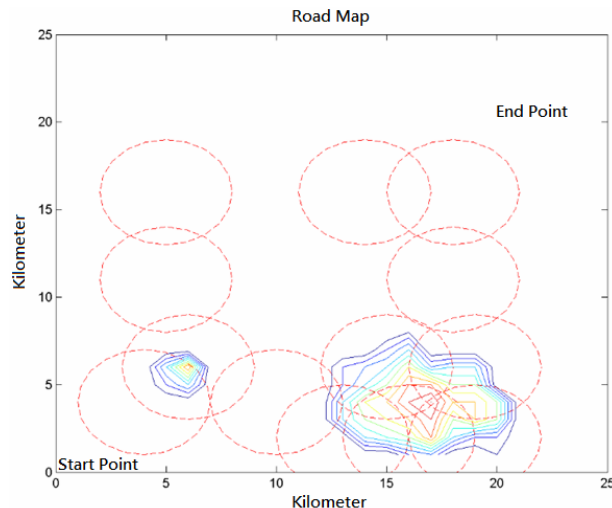
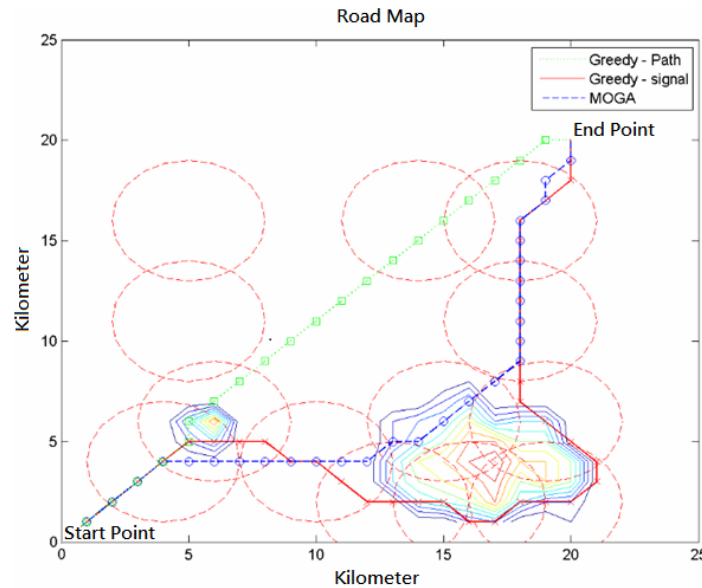


Fig. 8. Network topology of path planning case

The proposed MOGA is compared with the path-greedy and signal-greedy approaches in 0. Path planning results are captured in Fig. 9. It can be observed that the UAV of path-greedy algorithm almost straight flies from source point to destination point. Therefore, the flight route of path-greedy is the shortest. However, the UAV of path-greedy algorithm will pass through the middle area of this network topology, which is not covered by 3G communication signal. On the other hand, it can be observed that the UAV of signal-greedy flies based on 3G signal quality. Thereby, it results in the longest flight route. Unlike two greedy-based algorithms, the designed MOGA acquires the optimal flight route through evolution process. It can be observed that the MOGA not only shortens flight length but also achieves continuous data transmission compared to path-greedy and signal-greedy respectively.



**Fig. 9.** Flight route of three algorithms.

The planning results of two greedy-based algorithms and the proposed MOGA are compared in Table 2. Although the path length of proposed MOGA is slightly longer than the path-greedy algorithm, it achieves obviously better signal strength. Moreover, the path length of proposed MOGA is significantly shorter than the signal-greedy algorithm, and also achieves slightly better signal strength. The signal quality of proposed MOGA is 1.32 and 3.22 times relatively better than signal-greedy and path-greedy.

**Table 2.** Comparison of path planning results.

Algorithm	Path Length	Power / Distance
Path-greedy	27.2 (KM)	0.9 (mW)
Signal-greedy	42.6 (KM)	2.2 (mW)
MOGA	32.1 (KM)	2.9 (mW)

#### 4.2 Simulation Results

In simulation results, the performance of flight route is investigated and evaluated. In order to balance two objects, the weighted ratio of signal strength and path length is studied firstly. The signal cost and path cost versus weighted ratio of path to signal is captured in Fig. 10. Note that the crossing of signal curve and path curve represents the minimum cost of two objects. It can be observed that the minimum total cost is acquired when the weights of path length and signal strength are set to 0.37 and 0.63. Therefore, we set the variables  $\alpha$  and  $\beta$  of equation 6 to 0.37 and 0.63 in following simulations.

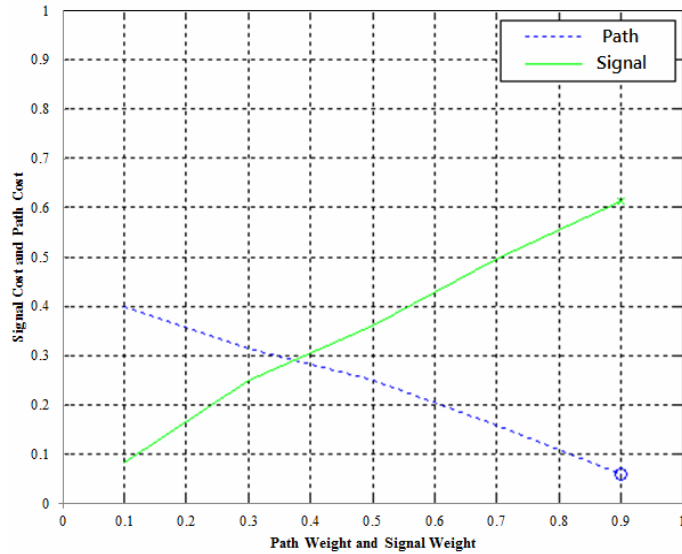


Fig. 10. Weight of path length and signal strength

The signal strength of three algorithms is captured in Fig. 11. The civil UAV starts its flight route from the coordinate point (1,1), so that there is no communication signal in the beginning. First of all, the received signal strength of civil UAV raises and falls because it approaches and leaves 3G BSs. It can be observed that the path-greedy algorithm achieves the shortest flight length and the signal-greedy algorithm results in the longest flight route. The proposed MOGA plans the shorter and longer flight route compared to the signal-greedy and path-greedy algorithms. In addition, the MOGA achieves the best signal quality during its flight router. It can be observed that the signal strength of three algorithms increases during flight path 3 to 7 km, because all of them fly the same route with the same signal strength in this section of flight route. However, the path-greedy algorithm loses communication signal from 12 km to 18 km of its flight route. It sacrifices signal strength for the shortest flight path. Both of signal-greedy and proposed MOGA sustain better signal strength around -100 to -40 dB during their flight routes. Moreover, the proposed MOGA yields the higher signal strength than the signal-greedy algorithm.

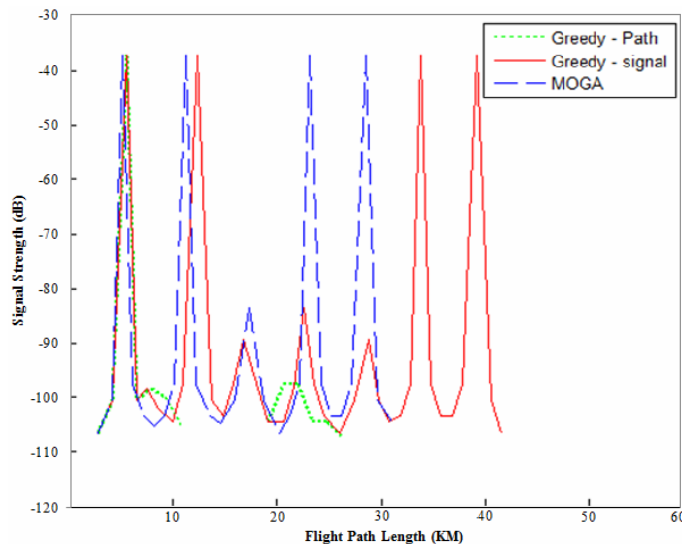
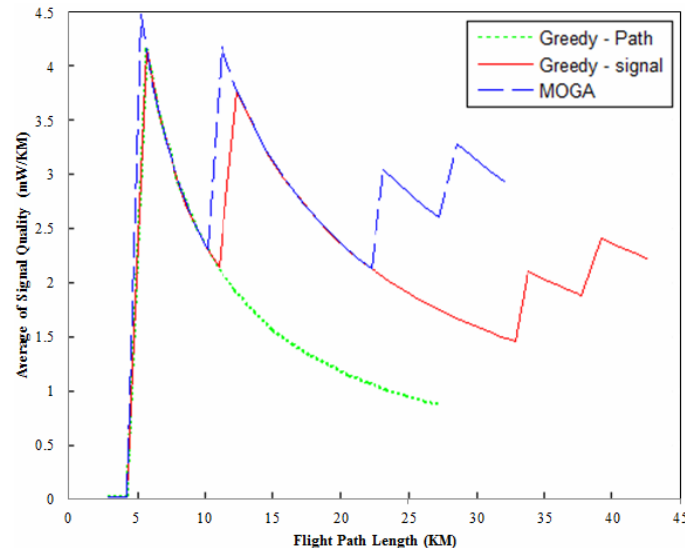


Fig. 11. Received signal strength during flight route

The average of signal quality during flight route is captured in Fig. 12. In the beginning of their flight routes, all algorithms achieve the similar average level of signal strength. It is attributed to the well coverage of 3G BSs from 0 to 5 km. After that, the average of signal quality decreases due to handover operation. It can be observed that the path-greedy algorithm receives the worst signal quality compared to

the proposed MOGA and signal-greedy algorithm. On the other hand, the proposed MOGA and signal-greedy algorithm yield the similar average level of signal quality. However, the proposed MOGA is superior to signal-greedy algorithm with slightly better average of signal quality and significantly shorter flight length. In summary, the path planning result of proposed MOGA yields the best signal quality and the shorter flight route compared to signal-greedy and path-greedy algorithms.



**Fig. 12.** Average signal quality of flight route

## 5 Conclusion and Future Work

In order to economize the expensive satellite communication, existing 3G communication networks are utilized to accomplish the data transmission of civil UAV in this paper. The proposed path planning approach with 3G communication networks not only avoids terrain obstacles but also considers communication quality. In addition, we have proposed a multi-objective Genetic algorithm to optimize the trade-off problem of path planning. The signal strength of 3G base stations and the path length of flight route are considered. Simulation results showed that the proposed MOGA yields the best signal strength and shorter path length compared to the signal-greedy and path-greedy algorithms. It not merely maximizes signal strength but minimizes the path length of flight route. In the future, we intend to consider more objects of path planning for civil UAVs and try to realize the proposed approach to realistic civil UAV environments.

## Acknowledgements

This work was partly funded by the Ministry of Science and Technology, Taiwan, R.O.C. under Grant no. MOST 103-2221-E-197-018 and 101-2221-E-197-008-MY3.

## References

- [1] S. Saripalli, J.F. Montgomery, G.S. Sukhatme, Visually guided landing of an unmanned aerial vehicle, *IEEE Transactions on Robotics and Automation* 19(3)(2003) 371-380.
- [2] J.-M. Chang, W.-T. Hsiao, J.-L. Chen, H.-C. Chao, Mobile relay stations navigation-based self-optimization handover mechanism in WiMAX Networks, in: *Proc. 2009 International Conference on Ubiquitous Information Technologies & Applications*, 2009.
- [3] F.-H. Tseng, H.-H. Cho, L.-D. Chou, H.-C. Chao, Efficient power conservation mechanism in spline function defined WSN

- terrain, *IEEE Sensors Journal* 14(3)(2014) 853-864.
- [4] Z. Sarris, Survey of UAV applications in civil markets, in: *Proc. 2001 Mediterranean Conference on Control and Automation*, 2001.
- [5] F.-H. Tseng, L.-D. Chou, H.-C. Chao, W.-J. Yu, Set cover problem of coverage planning in LTE-advanced relay networks, *International Journal of Electronic Commerce Studies* 5(2)(2014) 181-198.
- [6] D. Hausamann, W. Zirnig, G. Schreier, P. Strobl, Monitoring of gas pipelines: a civil UAV application, *Aircraft Engineering and Aerospace Technology* 77(5)(2005) 352-360.
- [7] D.B. Johnson, A note on dijkstra's shortest path algorithm, *Journal of the ACM* 20(3)(1973) 385-388.
- [8] M.-Y. Hsieh, Y.-M. Huang, H.-C. Chao, Adaptive security design with malicious node detection in cluster-based sensor networks, *Computer Communications* 30(11-12)(2007) 2385-2400.
- [9] H. Okcu, M. Soyuturk, Distributed clustering approach for UAV integrated wireless sensor networks, *International Journal of Ad Hoc and Ubiquitous Computing* 15(1/2/3)(2014) 106-120.
- [10] H.-B. Duan, Q.-X. Ding, S.-Q. Liu, J. Zou, Time-delay compensation of heterogeneous network control for multiple UAVs and UGVs, *Journal of Internet Technology* 11(3)(2010) 379-385.
- [11] J.-M. Chang, C.-C. Hsu, H.-C. Chao, J.-L. Chen, Design of dead-end-avoidance method for geographic forwarding in MANET, *Wireless Personal Communications* 61(4)(2011) 765-777.
- [12] K. Daniel, S. Rohde, C. Wietfeld, Leveraging public wireless communication infrastructures for UAV-based sensor networks, in: *Proc. 2010 IEEE International Conference on Technologies for Homeland Security*, 2010.
- [13] R. Miura, M. Maruyama, M. Suzuki, H. Tsuji, M. Oodo, Y. Nishi, Experiment of telecom/broadcasting mission using a high-altitude solar-powered aerial vehicle pathfinder plus, in: *Proc. 2002 International Symposium on Wireless Personal Multimedia Communications*, 2002.
- [14] X. Li, J. Xie, M. Cai, M. Xie, Z. Wang, Path planning for UAV based on improved heuristic A\* algorithm, in: *Proc. 2009 International Conference on Electronic Measurement & Instruments*, 2009.
- [15] T. Khuswendi, H. Hindersah, W. Adiprawita, UAV path planning using potential field and modified receding horizon A\* 3D algorithm, in: *Proc. 2011 International Conference on Electrical Engineering and Informatics*, 2011.
- [16] Z. Dong, Z. Chen, R. Zhou, R. Zhang, A hybrid approach of virtual force and A\* search algorithm for UAV path re-planning, in: *Proc. 2011 IEEE Conference on Industrial Electronics and Applications*, 2011.
- [17] S. Mittal, K. Deb, Three-dimensional offline path planning for UAVs using multiobjective evolutionary algorithms, in: *Proc. 2007 IEEE Congress on Evolutionary Computation*, 2007.
- [18] Z. Cheng, Y. Sun, Y. Liu, Path planning based on immune genetic algorithm for UAV, in: *Proc. 2011 IEEE Electric Information and Control Engineering*, 2011.
- [19] O. Castillo, L. Trujillo, P. Melin, Multiple objective genetic algorithms for path-planning optimization in autonomous mobile robots, *Soft Computing* 11(3)(2006) 269-279.
- [20] N. Sedaghat, Mobile robot path planning by new structured multi-objective genetic algorithm, in: *Proc. 2011 IEEE Soft Computing and Pattern Recognition*, 2011.
- [21] F.-H. Tseng, T.-T. Liang, C.-H. Lee, L.-D. Chou, H.-C. Chao, A star search algorithm for civil UAV path planning with 3G communication, in: *Proc. 2014 International Conference on Communications and Robotics Engineering*, 2014.
- [22] M.-H. Lin, X.-X. Zheng, The simulation and field measurement of cell planning scheme for WCDMA system, [thesis] Hualien, Taiwan: National Dong Hwa University, 2006.

[23] Telecom Technology Center, 2G and 3G mobile phone reception signal level supplement. <[http://freqgis.ncc.gov.tw/pub\\_new/Intro.aspx](http://freqgis.ncc.gov.tw/pub_new/Intro.aspx)>

[24] MATLAB, Overview. <<http://www.mathworks.com/products/matlab/html>>